Available online www.ejaet.com

European Journal of Advances in Engineering and Technology, 2020, 7(8):1-8

Research Article ISSN: 2394 - 658X

An analysis of the Influence of the Dielectric Substrate Parameters on the Performances of Koch and Minkowski Single-Iteration Fractal Antennas

David Vatamanu and Simona Miclaus

Department of Communications, Information Technology and Cyber Defence,"Nicolae Balcescu" Land Forces Academy, Sibiu, Romania
davidvatamanu@yahoo.com, simo.miclaus@gmail.com

ABSTRACT

Two simple printed fractal antennas were simulated in FEKO software with the aim of observing the influence of the dielectric substrate on their total efficiency and radiation patterns. The computations were made in the frequency range (0.5-3) GHz which is of interest for various wireless communication applications. Three types of dielectrics were investigated: an affordable material, the glass-reinforced FR-4 and two high-performance composite laminates made of Poly Tetra Fluoro Ethylene filled with glass or ceramic –duroid RT5880 and RO3003. Analyses on the obtained performances took into account: a) the nature of the dielectric substrate; b) its thickness; c) its area; d) the presence of other conductive material on the substrate. For example, RO3003 at 10 mm thick provided a maximum total efficiency of 88% of the Koch-1 antenna at a maximum realized gain of 6dBi. A usable bandwidth of 320 MHz could be achieved with this configuration while conditioning that total efficiency to always exceed 45%.

Key words: Fractal antenna, UHF communication, PTFE composite substrate, antenna performance, multi-band antenna

---

INTRODUCTION

In 1988 Nathan Cohen created the first self-similar shapes in the form of antenna elements while his finished designs were presented in 1995, inaugurating the fractal-antenna era [1-2]. Being multilevel and space filling conductive curves, and repeating a motif over two or more scale sizes called iterations, these antennas owe the specific property of highest compactness. They are used to provide multi- or wideband applications which are mostly appreciated in cellular, microwave- or body centric communications [3–18]. Very good performances could be identified with various models of antennas at different frequencies simultaneously while a series of performances were targeted during their design process analyses: miniaturization, band increase, multiple resonances achievement, high reliability and reduced costs. Some studies were focused on certain applications optimization. In general, fractal antennas developed for various applications in ultra- and super-high frequency bands are presently under continuous development.

A previous study of ours [19] focused on finding the best solution when deploying a point-to-point ultra-high frequency radio-link between two sites situated at 5.8 km distance, from the perspective of choosing the proper fractal antenna model. From six antenna models, the optimal ones have been chosen based on simulations. Present work aimed at a computational characterization of the functioning parameters of two simple fractal antennas (one-iteration) by modifying: a) the dielectric substrate material; b) the dielectric substrate thickness; c) the dielectric substrate area; d) the presence of small conductive materials on the substrate. To obtain the solutions we used the capabilities of antenna design and analysis provided by FEKO – Altair HyperWorks software. The final objective was to observe the influence other than antenna model itself on the performance of the antenna. Since the work is entirely based on simulation, present results have not yet been validated by measurements.

ANTENNA MODELS AND COMPUTATIONS

Antenna types

Koch-1 (one iteration) monopole and Minkowski-1 dipole (one iteration) printed antennas were analysed in the present approach (Fig. 1) over the frequency range (0.5-3) GHz. For Koch-1 antenna, all sides of the conductive wire had 3 cm length and for Minkowski-1antennathe side lengthshad1.5 cm each. The ground was set as a foil of perfect electric conductor (PEC) and the antenna wire was also made of PEC with a diameter of 1 mm. The dielectric substrate (used for printed circuit boards – PCB) was considered of three types: a) FR-4; b) Rogers RT5880; c) Rogers RO3003. FR-4 is an epoxy fibreglass sheet fire-resistant, a non-expensive material, which usually responds well up to frequencies of 1 GHz. Beyond this frequency its passive circuit elements start to count. It is most frequently used as a substrate of fractal antennas, being the cheapest solution. Composite RT/Duroid 5880 is a glass microfiber reinforced Poly Tetra Fluoro 100 Ethylene (PTFE) produced by Roger corporation. RO3003 laminates are ceramic-filled Poly Tetra Fluoro 104 Ethylene - 104 PTFE composite circuit materials with uniform mechanical characteristics regardless of the dielectric constant. These two composites are expensive but high-performance. In some other recent antenna designs, other composites such as Rogers RT/Duroid 5870 [10] or 6010 [13] have been checked as fractal antenna substrates. The materials chosen for present work have also been chosen in [18].

The first important parameter of the substrate is the dielectric constant, ε_r, which shows the material's ability to store electrical energy in the electric (E) field. Generally, ε_r varies with frequency but this was not taken into account in the present work. Some of the expensive dielectrics have ε_r which show much stable values over broader frequency ranges. Another important parameter is the dissipation factor (loss tangent), tanδ, which indicates how much losses appear when the wave propagates in the material. The lower tanδ is, the lower will be the dissipated power. It can also vary slightly with frequency, but in the present approach, it was considered constant over the entire frequency range of interest. For the dielectrics we used as substrates, the next parameters were set in the simulations over the (0.5-3) GHz: FR-4: ε_r=4.8, tanδ=0.017; RT5880: ε_r=2.2, tanδ=0.004; RO3003: ε_r=3.0, tanδ=0.0013.Three different thicknesses of the dielectric substrate were used in the simulations as well: d1=5mm; d2=7.5mm; d3=10mm. The dimensions of the substrate rectangle were 10x7.5cm^2, with the exception of some specific tests, when a modified area was introduced. The rest of the computational space was considered free space.

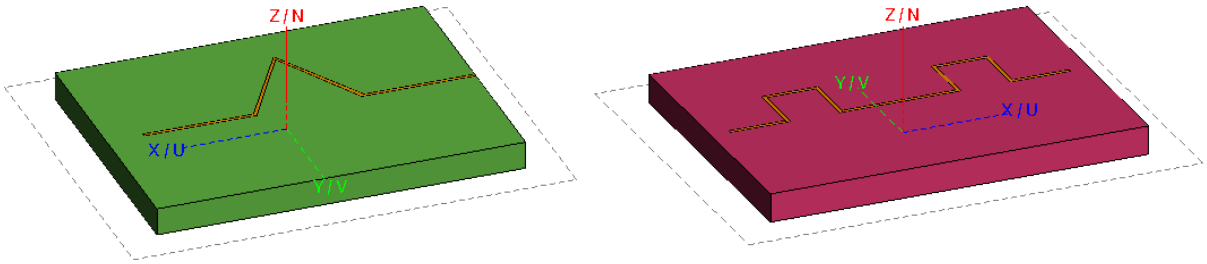

Fig. 1 Models of generated antennas on substrates: Koch-1 monopole antenna (left); Minkowski-1 dipole antenna (right)

Computation environment and investigated antenna characteristics

FEKO software from Altair HyperWorks uses the method of moments to compute the antenna currents and the electromagnetic fields. First, the geometry was built: the antennas wiring, the substrate and ground and the surrounding (free) space. Koch-1 monopole was fed on the edge, while Minkowski-1 dipole was fed in its center. A wire port was used as a source, and provided 1V at an impedance of 50 Ω. For computations of the far- and near-field solutions an input power of 1 W was set and a real impedance of 50 Ω. Discretization of the computational space made use of a standard mesh with a wire segment radius of 0.01. Triangular meshing was generated for the calculations and meshing size histograms can be observed in Fig. 2 for both antennas. Requesting the solution types and setting solution parameters was the next step.

Far field solution requests

Due to mismatches, reflexion may appear at the antenna feeding point and the parameter called Voltage Standing Wave Ratio (VSWR) is used to quantify this phenomenon. VSWR is mathematically connected to either the reflexion coefficient or to the return loss. VSWR = 1 means no reflexion exists, while higher values indicate presence of impedance mismatch and reflexion. Generally, the antenna bandwidth is defined as the frequency range for which the antenna exhibits a VSWR < 2:1 (which is equivalent with a return loss increase of 9.5 dBat the limits of the frequency band, reported to that of the centre frequency). In the case of present work, we imposed another condition to define the desired working bandwidths of interest. Knowing that the total efficiency of the antenna is the product between the radiation efficiency (the ratio between radiated power and forward power) and the mismatch efficiency (this one being directly connected to VSWR value), we established a chosen threshold of the total efficiency which fulfils our needs for the antennas: min. 45% of total efficiency will denote the limits of a working bandwidth in the present case. Also, in the computations we always represented the realized gain of the antenna since it takes into account the mismatch losses. Computation of the directivity and of the radiation patterns were also required from the solver.

Near field solution requests

The electric (E) and the magnetic (H) field components were also of interest in the very proximity of the antenna. Their magnitude map and instant vector fields' representations could be obtained, to have a complete view on the field- or power density distribution and orientation in space at distances not exceeding 3 wavelengths from the antenna.

Current request

Surface current and charge density were also computed in the conductive wires.

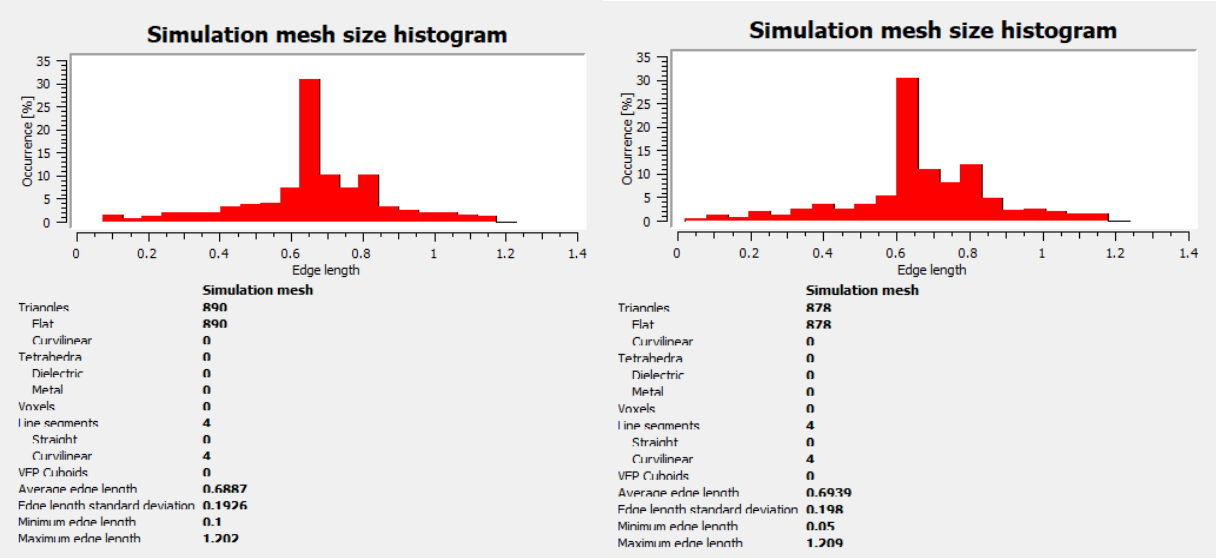

Fig. 2 Triangular meshing histograms of the computation space for the Koch-1 (left) and Minkowski-1 (right) antennas

SIMULATION RESULTS AND DISCUSSIONS

Reflexion Coefficient, Total Efficiency and Usable Bandwidths

Fig 3 shows the VSWR and the total efficiency variations with frequency forKoch-1and Minkowski-1 antennas printed on RO3003 composite substrate having two different thicknesses: 7.5 mm and 10 mm. Significant changes of both VSWR and total antenna efficiency can be observed when the substrate's thickness is modified. Also, in general only for frequencies larger than 2.55 GHz, VSWR becomes low enough so that the reflexion to be acceptable. At those frequencies, the efficiency exceeds 60% on some sub-bands for Koch-1 antenna and 40% respectively on others, for Minkowski-1 antenna. Mismatches decrease and total efficiency increase for the thicker substrate situation presented in Fig. 3.

A general view on the antennas VSWR, total efficiency and usable bandwidths with their dependencies on dielectric substrate type and on its thickness are summarized in Table 1 and Table 2 for Koch-1 and Minkowski-1 fractals respectively. The tables provide the values of these parameters, and in the situations for which the total efficiency was situated below 45% (the imposed threshold) an X mark was completed in the tables. The largest total efficiency (88 %) was provided by Koch-1 antenna printed on RO3003 substrate 10 mm thick. The respective VSWR was 1.19, and the usable bandwidth for which the efficiency was kept between (45-88) % was in the range (2.683-3) GHz. Frequencies larger than 3 GHz are expected to provide very good parameters, but they exceeded the objectives range of the present study.

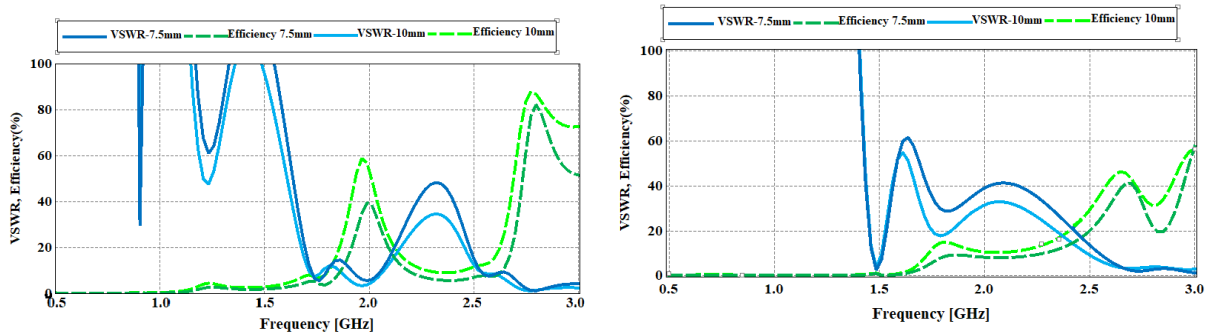

Fig. 3 Voltage standing wave ratio and total efficiency of Koch-1 (left) and Minkowski-1 (right) fractal antennas variation with frequency for the RO3003 composite substrate of two thicknesses: 7.5 mm and 10 mm

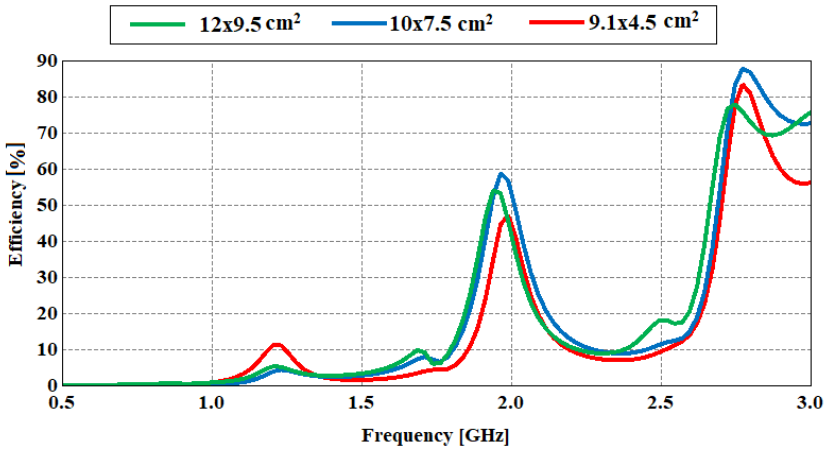

Fig. 4 The effect of substrate area modification on the total efficiency of Koch-1 antenna (substrate: RO3003, d3=10mm): blue curve = initial antenna (10x7.5cm^2); green curve=enlarged area (12x9.5cm^2); red curve=diminished area (9.1x4.5cm^2)

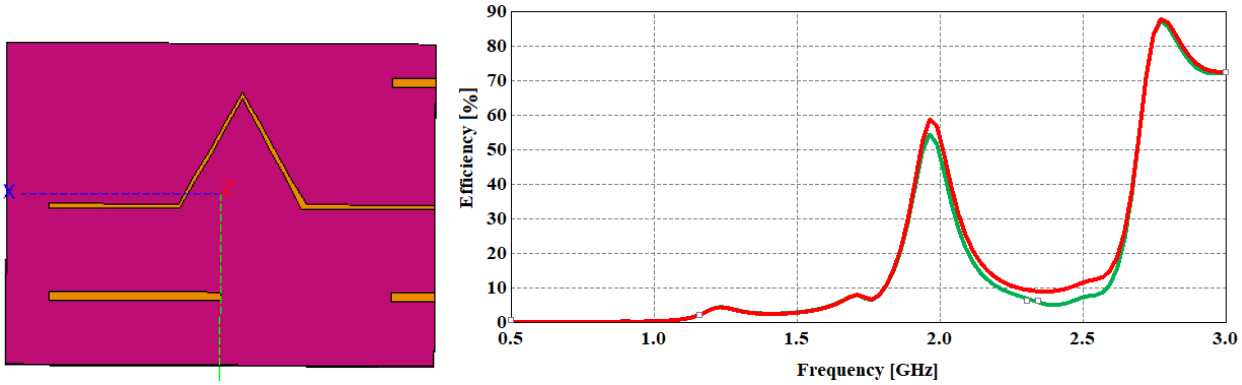

Fig. 5 The effect of presence of other conductive wires on the substrate of RO3003, 10 mm thick, on the total efficiency of Koch-1 antenna: red curve is initial antenna case, green curve indicates efficiency modified by the presence of other conductive material nearby

Fig. 4 indicates the effect of the substrate area modification on the total efficiency of the antenna. The case of Koch-1 antenna on a 10 mm thick substrate of composite RO3003 is exemplified and it is observed that the dielectric area has different effect at different frequencies. Interesting to mention is that at resonance frequencies variations of the total efficiency of up to 15% were observed and at 3 GHz even larger variations were achieved due to small modifications of the substrate area. Fig. 5 demonstrates the effect of presence of other small conductive wires besides the antenna itself, on the substrate. On the left side of Fig. 5 the presence of three extra horizontal wires is observed, while on the right side the effect of their presence on the total efficiency is depicted. In case of this Koch-1 antenna with RO3003 substrate of 10 mm thick, the maximum shift of efficiency reaches 4.5%, as observed. Therefore, near-field perturbation by other conductive material will change the initial designed parameters of the antenna as well.

Table -1 Koch-1 fractal antenna with the parameters and usable bands defined by a total efficiency > 45%, in function of the substrate material and thickness

Substrate thickness	**5mm**			**7.5mm**			**10mm**		
Substrate type	**Return Loss**	**Band-width**	**Efficiency**	**Return Loss**	**Band-width**	**Efficiency**	**Return Loss**	**Band-width**	**Efficiency**
FR-4	X	X	X	27.5dB	2299-2345 MHz	46.8%	21dB	2238-2861 MHz	69%
				31dB	2565-2839 MHz	50%			
RO3003	9dB	2780-2880 MHz	60%	19.6dB	2728-3000 MHz	82%	5.2dB	1923-2025 MHz	59%
							21.3dB	2683-3000	88%
RT5880	X	X	X	4.4dB	2231-2272 MHz	47.3%	7.3dB	2155-2290 MHz	66.5%

Table -2 Minkowski-1 fractal antenna with the parameters and usable bands defined by a total efficiency > 45%, in function of the substrate material and thickness

Substrate thickness	5mm			7.5mm			10mm		
Substrate type	**Return Loss**	**Band-width**	**Efficiency**	**Return Loss**	**Band-width**	**Efficiency**	**Return Loss**	**Band-width**	**Efficiency**
FR4	X	X	X	X	X	X	7.8dB	2141-2208 MHz	46.6%
							7.2dB	2421-2488 MHz	46.5%
RO3003	X	X	X	17.1dB	2959-3000 MHz	58%	5.5dB	2620-2680 MHz	46.3%
							6.6dB	2911-3000 MHz	56.4%
RT5880	X	X	X	X	X	X	X	X	X

Antennas Gain, Radiation Pattern, Near Field and Current Distribution

Fig. 6 presents the realized gain of the two antennas in function of frequency for 10 mm thick substrate RO3003. Elevation angle is θ = 0 along Oz axis and azimuth angle is φ= 0 along Ox axis. Two maxima are observable on the realized gain curves and at those frequencies, separate complete 2D radiation patterns in azimuth and elevation are presented in the micro-windows on the graphs.

A synopsis of maximum realized gains in function of substrate material and thickness is presented in Table 3 and 4 for Koch-1 and Minkowski-1 antenna respectively. The three values of the realized gains correspond to the frequencies of the usable bands presented in Tables 1 and 2, namely to the lowest/center/highest efficiency-corresponding frequency. The highest realized gains are in the range (7.5-8) dBi and they also depend on the substrate type and thickness.

Fig. 7 and Fig. 8 show the radiation patterns of the fractal antennas at various frequencies and with different substrate parameters. The realized gain distribution may be observed. Antenna position relative to the obtained pattern is also visually provided. The chosen cases indicate the higher or smaller directivity available with these configurations. Large radiation lobes are generally observed for the chosen cases, so they are low-directive. Fig. 9 allows visualization, at a specific frequency, of the E- and H-field strengths distributions on the surface of the substrate, in air, nearby Koch-1 antenna. The substrate was composite RO3003 of 10 mm thick. In the E-field representation, a maximum is observed at the feeding wire port, of 120 kV/m. This field level corresponds to an input power of 1 W in the antenna. At the exemplified frequency of 1.914 GHz, Koch-1 fractal showed a total efficiency of 59%. As expected, H-field was not in phase with E-field. Fig. 10 presents a vectorial description of an instant of the near-field evolution at the surface of the substrate/antenna Koch-1. Flux densities of E- and H-field

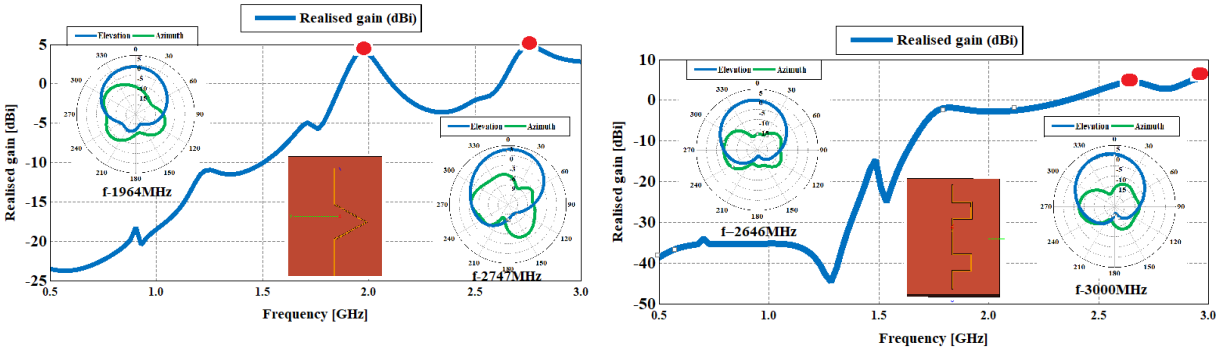

Fig. 6 Realized gain of Koch-1 (left) and Minkowki-1(right) antennas in function of frequencyonRO3003 substrate 10 mm thick together with respective radiation patterns at selected frequencies in elevation (φ= 90°) and azimuth (θ= 90°).

Table -3 Koch-1 fractal antenna with maximum realized gains (in dBi) corresponding to the lower/center/upper limits of the frequency bands, in function of the substrate material and thickness

Substrate thickness/type	5mm			7.5mm			10mm		
FR-4	X	X	X	2.5dBi	3dBi	3dBi	5dBi	3dBi	6dBi
				3dBi	3dBi	3dBi			
RO3003	6dBi	5dBi	6dBi	4dBi	6dBi	7.5dBi	5dBi	6dBi	6dBi
							4dBi	6dBi	7.5dBi
RT5880	X	X	X	6dBi	6dBi	6dBi	5dBi	4dBi	6dBi

Table -4 Minkowski-1 fractal antenna with maximum realized gains (in dBi) corresponding to the lower/center/upper limits of the frequency bands, in function of the substrate material and thickness

Substrate thickness/type	5mm			7.5mm			10mm		
FR4	X	X	X	X	X	X	6dBi	6dBi	6dBi
							6dBi	5dBi	5dBi
RO3003	X	X	X	6dBi	8dBi	8dBi	5dBi	5dBi	5dBi
							6dBi	8dBi	8dBi
RT5880	X	X	X	X	X	X	X	X	X

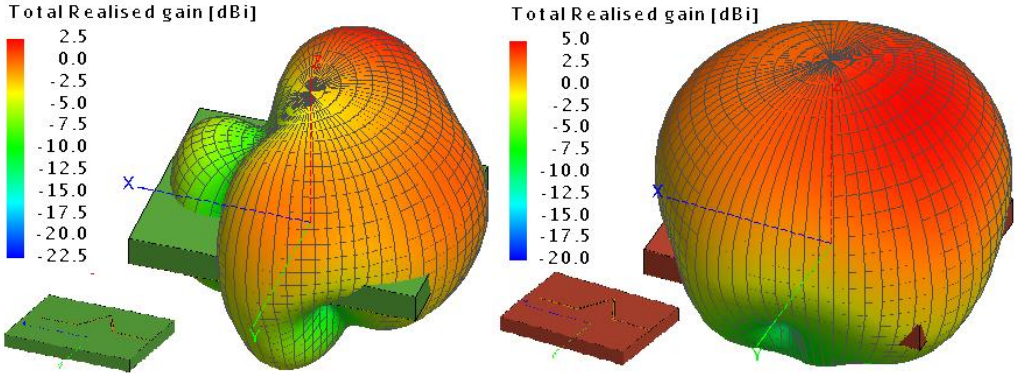

Fig. 7 Radiation patterns of Koch-1 antennas: substrate FR-4, 10 mm thick at 3 GHz (left); substrate RO3003, 10 mm thick at 2.898 GHz (right)

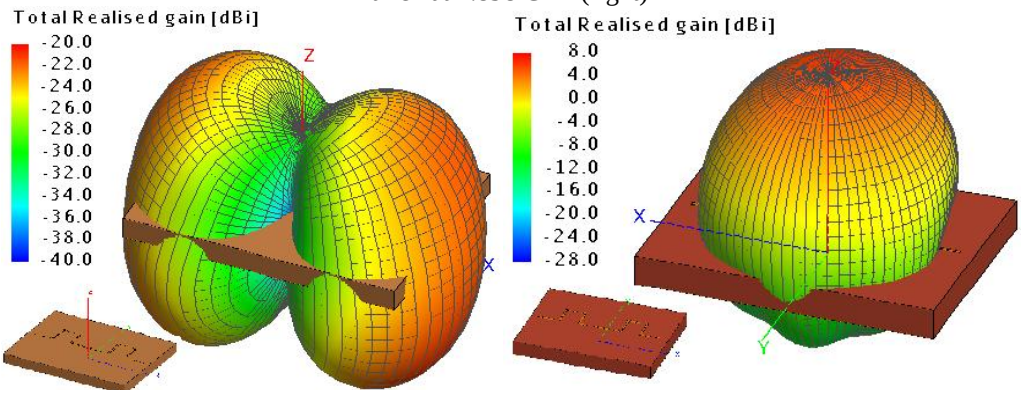

Fig. 8 Radiation patterns of Minkowski-1 antennas: substrate RT5880, 7.5 mm thick at 1.535 GHz (left); substrate RO3003 10 mm thick at 3 GHz (right)

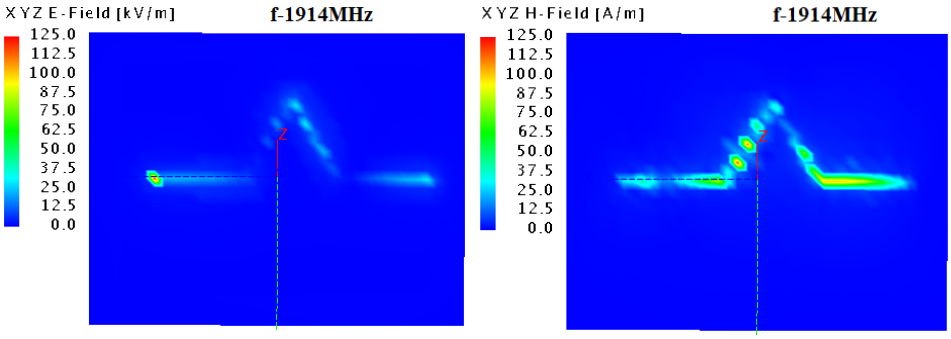

Fig. 9 Near-field of Koch-1 antenna with substrate RO3003, 10 mm thick, in the plane of substrate surface: E-field strength (left); H-field strength (right), at input power of 1 W

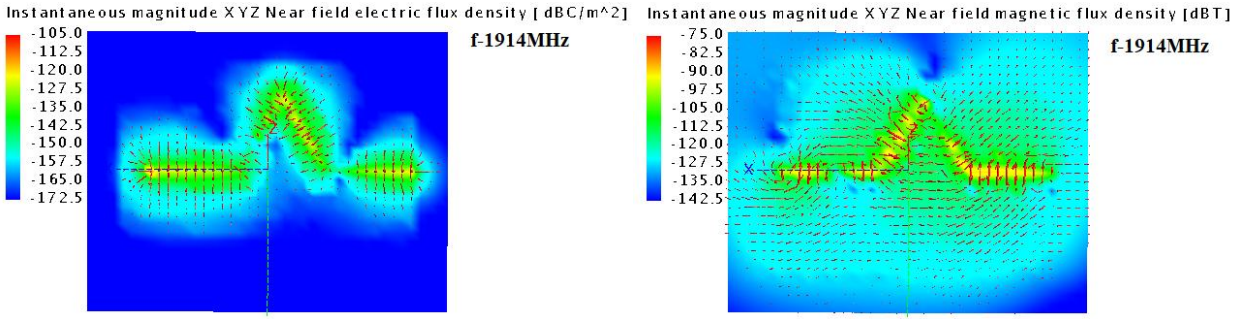

Fig. 10 Instantaneous vector near-field distribution for Koch-1 antenna with substrate RO3003, 10 mm thick, in the plane of substrate surface: electric field density vectors (left); magnetic field density vectors (right), at input power 1 W

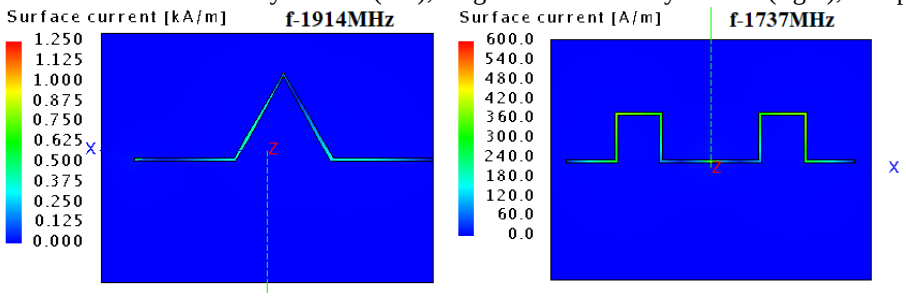

Fig. 11 Surface current distribution along the wire fractal antennas Koch-1 (left) and Minkowski-1 (right) at specific frequencies, with RO3003 substrate, 10 mm thick when input power was 1 W

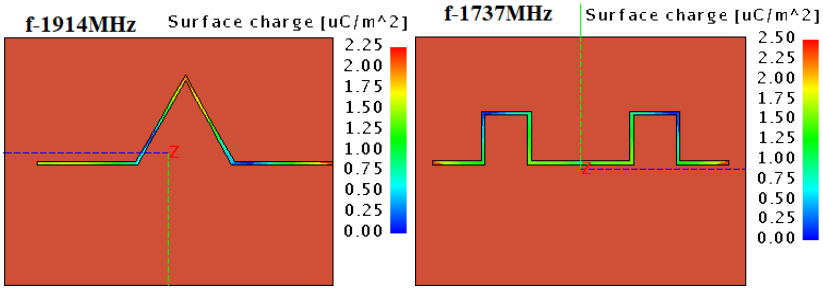

Fig. 12 Charge density distribution along the wire fractal antennas Koch-1 (left) and Minkowski-1(right) at specific frequencies, with RO3003 substrate, 10 mm thick, at input power 1 W

Vectors are visualized and their magnitude is indicated, when the input power was also 1 W. In Fig. 11 the description of the surface current along both fractal antennas is figured, at two different frequencies. Similarly, Fig. 12 shows the surface charge density for the same situations. In both cases the substrate was composite RO3003 of 10 mm thick and the input power in the antennas was 1 W. It may be seen that maximum magnitudes of surface currents are very different for the two frequencies and antennas, while the surface charge density spreads in the same limits for both antennas and frequencies. Many of the situations exemplified in images above referred to the substrate made of composite RO3003 because it provided, for the present two antenna types, the best performances.

CONCLUSION

Present paper aimed at a detailed analysis of the dielectric substrate's influence on the main working parameters of two simple models of printed fractal antennas. The capabilities of simulations offered by FEKO – Altair HyperWorks software were used. With the considered cases of one-iteration antennas having a side of 1.5 or 3 cm, it was proved that the usable frequencies successfully exceed 2.5 GHz, which is of great interest for nowadays configurations of wireless communication devices. The antennas offered realized gains of up to 8 dBi and total efficiencies of maximum 88%, when multi-band applications are considered. The main results however were focused on observing how the material of the dielectric substrate on which the antenna conductive wire is printed, its thickness and its area, influence the characteristics of the antenna. Indeed, all three parameters have significant impact on all characteristics, which means that the design and production has to carefully take into account all these factors. In our cases, doubling the substrate thickness or changing the material's dielectric parameters conducted to changes of even 28 % of the total efficiency, modifying the maximum realized gain with even 2.5 dB and sometimes tripling the usable bandwidth (defined by a minimum threshold of 45 % imposed to the total efficiency). The area of the dielectric substrate impacted with up to 15 % the total efficiency at resonance frequencies, at a change of 12-15 %. Also, the presence of even small amount of conductive materials nearby the antenna affects its designed performance.

REFERENCES

[1]. C Puente, J Romeu, R Pous, A Cardama, Multiband Fractal Antennas and Arrays. Fractals in Engineering. Springer, London, pp. 222-236, 1997.

[2]. J Anguera, A Andújar, J Jayasinghe, VVS Sameer Chakravarthy, PSR Chowdary, T Ali, JLPijoan, C Cattani, Fractal Antennas: An Historic Perspective, *Fractal and Fractional*, 2020, 4(1):3.

[3]. MNA Karim, MKA Rahim, T Masri, O Ayop, Analysis ofFractal Koch Dipole Antenna for UHF band application, *2008 IEEE International RF and Microwave Conference*, Kuala Lumpur, 2008, 318-321.

[4]. RK Kanth, AK Singhal, P Liljeberg, H Tenhunen, Design of multiband fractal antenna for mobile and handheld terminals, *2009 First Asian Himalayas International Conference on Internet*, Kathmandu, 2009, 1-4.

[5]. MNA Karim, MK Abd Rahim, HA Majid, OB Ayop, M Abu, F Zubir, Log Periodic Fractal Koch Antenna for UHF Band Applications, *Progress in Electromagnetics Research*, 2010, Vol. 100, 201-218.

[6]. AMA Sabaawi, KM Quboa, Design and fabrication of miniaturized fractal antennas for passive UHF RFID tags, in: Advanced Radio Frequency Identification Design and Applications, Dr Stevan Preradovic, Ed. InTech, 2011.

[7]. A Kuar, N Saluja, JSUbhi, A hexagonal multiband fractal antenna used for wireless applications, *International Journal of Electronics and Computer Science Engineering*, 2012, 1(4), 2107-2111.

[8]. MA Dorostkar, MT Islam, R Azim, Design of a Novel Super Wide Band Circular-Hexagonal Fractal Antenna, *Progress in Electromagnetics Research*, 2013, Vol. 139, 229-245.

[9]. MEB. Jalil, MK Abd Rahim, NA Samsuri, NA Murad, HA Majid, K Kamardin, M Azfar Abdullah, Fractal Koch Multiband Textile Antenna Performance with Bending, Wet Conditions and on the Human Body, *Progress In Electromagnetics Research*, 2013, Vol. 140, 633-652.

[10]. OM Khan, ZU Islam, I Rashid, FA Bhatti, QU Islam, Novel Miniaturized Koch Pentagonal Fractal Antenna for Multiband Wireless Applications, *Progress In Electromagnetics Research*,2013, Vol. 141, 693-710.

[11]. NS Dandgavhal, MB Kadu, RP Labade, Bandwidth and Gain Enhancement of Multiband Fractal Antenna using Suspended Technique, *European Journal of Advances in Engineering and Technology*, 2015, 2(7), 38-42.

[12]. P Dupte, M Mathpati, Design and Simulation of Koch FractalAntenna for UWB Applications, *International Journal of Innovative Research in Computer and Communication Engineering*, 2018, 6(7), 7013-7018.

[13]. S Gupta, P Kshirsagar, B Mukherjee, Sierpinski fractal inspired inverted pyramidal DRAfor wide band applications, Electromagnetics, *Taylor & Francis*, 2018, 38(2), 103–112.

[14]. T Benyetho, J Zbitou, L El Abdellaoui, H Bennis, A Tribak, A New Fractal Multiband Antenna for Wireless Power Transmission Applications, *Active and Passive Electronic Components*, 2018, 3, 1-10.

[15]. E Jayapal, S Varadarajan, Design and Analysis of Sierpinski Carpet Fractal Antenna for UHF Spaced Antenna Wind Profiler Radar, *International Journal of Innovative Technology and Exploring Engineering*, 2019, 9(1), 839-842.

[16]. M Salucci, N Anselmi, S Goudos, A Massa, Fast design of multiband fractal antennas through a system-by-design approach for NB-IoT applications, *EURASIP J. Wireless Comm. Network*, 2019, 2019(1), pp. 1-15.

[17]. D Tumakov, D Chikrin, P Kokunin, Miniaturization of a Koch-Type Fractal Antenna for Wi-Fi Applications, *Fractal and Fractional*, 2020, 4(2):25.

[18]. YIA. Al-Yasir, MK Alkhafaji, HA Alhamadani, NO Parchin, I Elfergani, AL Saleh, J Rodriguez, RA Abd-Alhameed, A New and Compact Wide-Band Microstrip filter-Antenna Design for 2.4 GHz ISM Band and 4G Applications, *Electronics*, 2020, 9(7), 1084.

[19]. D Vatamanu, S Miclaus S, UHF Fractal Antennas: Solutions for Radio Links Using Matlab Simulations, *International Conference Knowledge-Based Organization*, Sibiu, Romania, 2020, Vol. XXVI, No. 3.